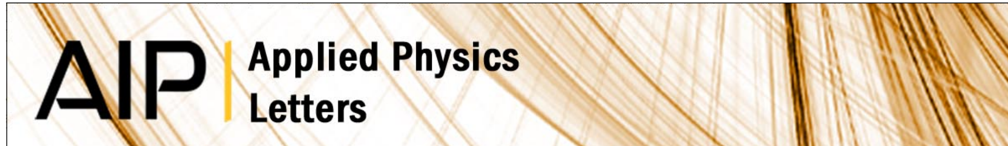

Suppression of planar defects in the molecular beam epitaxy of GaAs/ErAs/GaAs heterostructures

Adam M. Crook, Hari P. Nair, Domingo A. Ferrer, and Seth R. Bank

Citation: Appl. Phys. Lett. 99, 072120 (2011); doi: 10.1063/1.3626035
View online: http://dx.doi.org/10.1063/1.3626035
View Table of Contents: http://apl.aip.org/resource/1/APPLAB/v99/i7
Published by the American Institute of Physics.

Related Articles

Polarization Coulomb field scattering in In0.18Al0.82N/AlN/GaN heterostructure field-effect transistors
J. Appl. Phys. 112, 054513 (2012)

Modulation doping to control the high-density electron gas at a polar/non-polar oxide interface
Appl. Phys. Lett. 101, 111604 (2012)

Ultra low-resistance palladium silicide Ohmic contacts to lightly doped n-InGaAs
J. Appl. Phys. 112, 054510 (2012)

Enhancement of electrical conductivity of thick silver electrode using a tailored amorphous alloy
Appl. Phys. Lett. 101, 084104 (2012)

Nanoscale contacts between semiconducting nanowires and metallic graphenes
Appl. Phys. Lett. 101, 063122 (2012)

Additional information on Appl. Phys. Lett.

Journal Homepage: http://apl.aip.org/
Journal Information: http://apl.aip.org/about/about_the_journal
Top downloads: http://apl.aip.org/features/most_downloaded
Information for Authors: http://apl.aip.org/authors

ADVERTISEMENT

Downloaded 15 Sep 2012 to 128.83.63.20. Redistribution subject to AIP license or copyright; see http://apl.aip.org/about/rights_and_permissions

Suppression of planar defects in the molecular beam epitaxy of GaAs/ErAs/GaAs heterostructures

Adam M. Crook,[a] Hari P. Nair, Domingo A. Ferrer, and Seth R. Bank
Electrical and Computer Engineering Department, Microelectronics Research Center, The University of Texas at Austin, 10100 Burnet Rd. Bldg. 160, Austin, Texas 78758, USA

(Received 13 June 2011; accepted 27 July 2011; published online 19 August 2011)

We present a growth method that overcomes the mismatch in rotational symmetry of ErAs and conventional III-V semiconductors, allowing for epitaxially integrated semimetal/semiconductor heterostructures. Transmission electron microscopy and reflection high-energy electron diffraction reveal defect-free overgrowth of ErAs layers, consisting of $>2\times$ the total amount of ErAs that can be embedded with conventional layer-by-layer growth methods. We utilize epitaxial ErAs nanoparticles, overgrown with GaAs, as a seed to grow full films of ErAs. Growth proceeds by diffusion of erbium atoms through the GaAs spacer, which remains registered to the underlying substrate, preventing planar defect formation during subsequent GaAs growth. This growth method is promising for metal/semiconductor heterostructures that serve as embedded Ohmic contacts to epitaxial layers and epitaxially integrated active plasmonic devices. © *2011 American Institute of Physics*. [doi:10.1063/1.3626035]

Metal/semiconductor heterostructures are integral to the operation of every optoelectronic device. In addition to the conventional role as Ohmic or Schottky contacts, integration of metals within optical devices has received substantial attention, due to the strong confinement of light that can be achieved at metal-dielectric interfaces.[1] In particular, surface plasmon modes at these interfaces are promising for scaling photonic devices, enhancing semiconductor absorption and emission, as well as improving the sensitivity of biological sensors. However, metals remain relegated to the device periphery, due to the lack of a suitable material system for 3D integration. As such, complex plasmonic structures, such as a light source surrounded by metallic films are exceedingly challenging to fabricate with conventional methods.[2] An epitaxial approach to metal/semiconductor integrated devices would offer new paradigms for the design and fabrication of plasmonic devices.

Several epitaxial metal/semiconductor systems have been investigated, initially motivated by application to metal-base transistors[3]; however, a suitable prototype material system has not yet been demonstrated, due to issues including interfacial stability and epitaxial compatibility that must be simultaneously satisfied. The rare-earth monopnictides (RE-V) and conventional III-V semiconductors (e.g., GaAs) are promising for demonstration of epitaxial metal/semiconductor heterostructures. We will focus on the ErAs/GaAs material system due to the maturity of ErAs growth. ErAs is semimetallic with bulk resistivity of 70 $\mu\Omega$-cm.[4] When grown on GaAs, the interface is thermodynamically stable[5] and the cubic lattice constants for zinc blende GaAs and rocksalt ErAs only differ by 1.6%. Additionally, alloys of semimetallic $Sc_{1-x}Er_xAs$ have been grown lattice-matched to GaAs.[6] Unfortunately, early attempts to integrate ErAs films into GaAs resulted in highly defective GaAs overgrowth of the ErAs films.[4] The defects form due to the islanding growth mode of GaAs grown on ErAs, as well as the mismatch in rotational symmetry of the crystal structures.[7] In order to realize the full potential of ErAs/GaAs heterostructures—and RE-V/III-V materials more broadly—full films must be embedded without compromising overgrowth quality. In this letter, we address this limitation with a growth method that enables the embedding of ErAs layers in GaAs, without the formation of planar defects that have historically plagued the material system. Transmission electron microscopy (TEM) was employed to characterize planar defects in GaAs overgrowth, as well as the interface roughness and uniformity of the ErAs layers.

Various applications have motivated research groups to examine erbium incorporation into GaAs under differing growth conditions. Codeposition of erbium and GaAs (Refs. 8–12) can be summarized by the following growth model: at low erbium fluxes, erbium segregates to the growth surface (illustrated in Fig. 1(a)) and incorporation is limited by growth kinetics; with increasing erbium flux, the surface erbium concentration exceeds a critical areal density for nanoparticle formation and ErAs precipitates form (Fig. 1(b)); surface erbium that can diffuse to the ErAs nanoparticles will preferentially incorporate resulting in larger particles or extended structures. Several experimental results support this growth model. Low erbium fluxes resulted in substitutional incorporation;[8] however, at higher erbium fluxes, the erbium incorporated in interstitial sites, which TEM revealed to be rocksalt ErAs precipitates.[9] Even for layers with high Er-doping, there was a distinct gap between the interface of the erbium-containing layer and the appearance of the first ErAs precipitates.[13] The morphology of the ErAs precipitates was modified with the growth conditions, such that extended structures were realized for the highest erbium surface mobility.[13] The nanoparticle growth regime[12–16] can be thought of as an extension of the high erbium-doped growth. In this case, a layer of nanoparticles, usually $<50\%$ surface coverage, is intentionally deposited at the GaAs surface. The exposed GaAs surface acts as a seed for the overgrowth, avoiding the mismatch in rotational

[a]Author to whom correspondence should be addressed. Electronic address: acrook@mail.utexas.edu.

 © 2011 American Institute of Physics

Downloaded 15 Sep 2012 to 128.83.63.20. Redistribution subject to AIP license or copyright; see http://apl.aip.org/about/rights_and_permissions

FIG. 1. (Color online) Illustration of the nanoparticle-seeded film growth method for embedding ErAs in GaAs. (a) At the initiation of an erbium flux, erbium segregates to the surface. (b) ErAs nanoparticles form when the surface concentration exceeds the critical areal density. (c) Exposed GaAs seeds the overgrowth of the nanoparticles resulting in a single-phase spacer. (d) Erbium diffuses through the spacer and incorporates at the nanoparticle seed layer. The layer grows laterally until it coalesces into a film. The GaAs spacer maintains the symmetry of the substrate and seeds subsequent III-V film growth.

symmetry (Fig. 1(c)).[15,16] Few applications have required simultaneous investigation into the two distinct incorporation regimes. However, recent attempts to integrate ErAs nanostructures within optical devices[17] have required reduction in parasitic erbium incorporation (previously observed by Jourdan *et al.*[14]). It was shown that the key parameter to achieve high optical quality III-V material above the ErAs layers is the amount of GaAs overgrowth between the ErAs nanoparticle layer and the surface while cooling the erbium cell.[17] This demonstrated the propensity of subsurface ErAs nanoparticles to scavenge erbium atoms adsorbed on the surface, which is the foundation of the nanoparticle-seeded growth method.

Figure 1 illustrates the nanoparticle-seeded growth method. Growth began with embedding an ErAs nanoparticle seed layer in GaAs via the conventional method and overgrowing with a thin GaAs spacer layer of thickness t_{sp} (Fig. 1(c)). The sample was then heated to 600 °C to enhance erbium diffusion, and the erbium flux was reinitiated to grow the buried ErAs nanoparticles into a full film. Because of the low erbium flux, surface erbium diffused through the GaAs spacer and preferentially incorporated at the subsurface nanoparticles without building up sufficient surface concentration to nucleate ErAs nanoparticles on the GaAs surface. The underlying nanoparticles expanded laterally until they coalesced into a film (Fig. 1(d)). Because the film was grown through a thin GaAs spacer that was seeded by the substrate, the zinc blende symmetry was maintained and subsequent GaAs overgrowth was single-phase.

Samples were grown by molecular beam epitaxy on semi-insulating GaAs (100) substrates. The sample structure consisted of five ErAs films, each with 5 ML total ErAs deposition, embedded in GaAs. Growth details of the nanoparticle seed layer, which consisted of 1.33 ML ErAs, are given elsewhere.[17] Subsequent ErAs was grown with the erbium cell cooled to 920 °C, top produce a flux of $\sim 8 \times 10^{12}$ cm^{-2}s^{-1} (0.0123 ML/s effective growth rate). The GaAs spacer thickness was progressively increased from 1–3 nm, which is a range that was expected to be favorable for erbium diffusion to the subsurface ErAs. The top film was grown without a GaAs spacer layer, corresponding to the conventional layer-by-layer growth method. A 100 nm GaAs layer was grown after each ErAs film to ensure a smooth starting surface for the subsequent ErAs film. The structure was examined with cross-sectional TEM using a 200 kV FEI Tecnai TF20 instrument. A TEM image of the sample is shown in Fig. 2. The GaAs spacer thickness (t_{sp}) is overlaid on each ErAs layer. The surface was monitored *in situ* with reflection high-energy electron diffraction (RHEED). A streaky GaAs 2 × 4 reconstruction was observed prior to the growth of each ErAs layer. Degradation of the GaAs overgrowth was only observed for the final ErAs film that was grown with a 0 nm spacer (i.e., the conventional growth method).

The high-resolution (HR) TEM images of the top and bottom ErAs films are shown in Fig. 3. The GaAs overgrowth of the conventionally grown film (Fig. 3(a)) clearly shows planar defects, consistent with twinning and antiphase domains, that are expected to form during the overgrowth of the rock-salt ErAs with the zinc blende GaAs.[18] By contrast, as shown in Fig. 3(b), the GaAs overgrowth of the nanoparticle-seeded film, grown through a 1 nm GaAs spacer, exhibited no such planar defects. This corresponds to over twice the total erbium deposition that can be grown by the conventional method without the degradation in the GaAs overgrowth,[19] validating the new growth physics. Careful inspection of the nanoparticle-seeded film indicated a modest increase in roughness and decrease in homogeneity of the ErAs film, as compared to those grown by the conventional method.

The HR-TEM images of the films grown with thicker GaAs spacer layers reveal the importance of the capping layer thickness in the nanoparticle-seeded growth method. The GaAs spacer thickness must be carefully chosen to be thin enough to sink the Er efficiently, but thick enough that it maintains a sufficiently continuous GaAs film to prevent planar defect formation. With increasing GaAs spacer thickness, we observed the appearance of a second nanoparticle layer and decreasing uniformity of the "film" grown at the

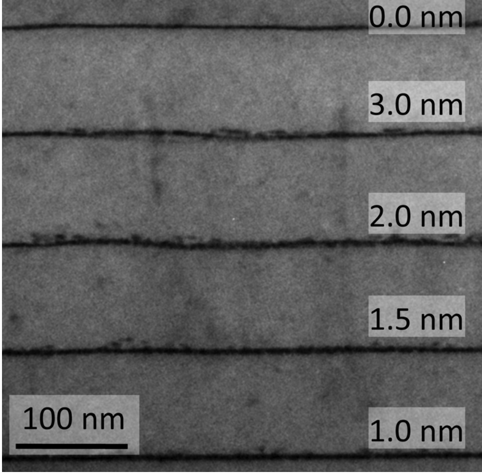

FIG. 2. Cross-section TEM image of the ErAs layers. The spacer thickness (t_{sp}) for each film is overlaid on the image.

Downloaded 15 Sep 2012 to 128.83.63.20. Redistribution subject to AIP license or copyright; see http://apl.aip.org/about/rights_and_permissions

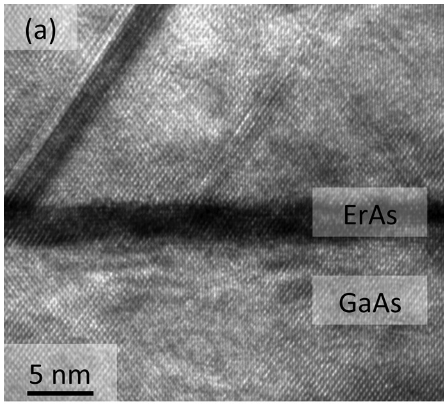

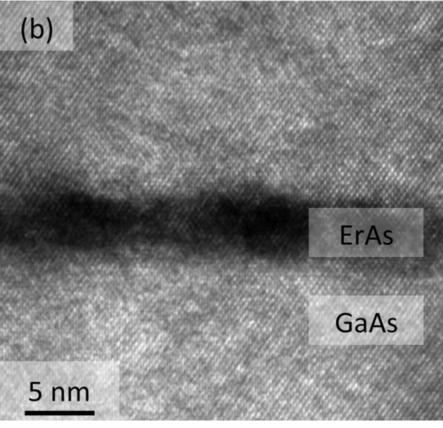

FIG. 3. High-resolution TEM images of (a) conventionally grown ErAs layer and (b) nanoparticle-seeded ErAs layer grown through 1.0 nm GaAs spacer.

nanoparticle seed layer. Figure 4 shows the HR-TEM image for the nanoparticle-seeded film grown with a 3 nm GaAs spacer. It is clear that the nanoparticle-seed layer (denoted lower) has not coalesced into a film prior to the formation of a second ErAs nanoparticle layer on the surface of the GaAs spacer (denoted upper). It is important to note, however, that the total erbium deposition at the surface during the film growth was 3.67 ML. This is more than the $\sim$2 ML of ErAs nanoparticles that can be overgrown at the elevated growth temperature, without resulting in highly defective GaAs overgrowth. This implies that some of the erbium diffused to the nanoparticle-seed layer to incorporate prior to the formation of the surface nanoparticle layer. Additionally, in each of the ErAs films grown with $>$1.0 nm GaAs spacers, we observed two distinct nanoparticle layers. It is important to note that we did not observe pillars, or similar features, that connected the nanoparticle-seed layers to the surface, which one might expect if the nanoparticles had a tendency to expand vertically. This is particularly promising for the future development of the film growth technique as it implies that it is favorable for the subsurface nanoparticles to expand laterally, resulting in a quasi-layer-by-layer growth mechanism.

In conclusion, we have presented a growth method that has the potential to overcome the mismatch in rotational symmetry that has precluded the integration of rare-earth monopnictide films with high-quality III-V materials. The method was applied to the ErAs/GaAs prototype material system where we utilized the two distinct growth regimes of

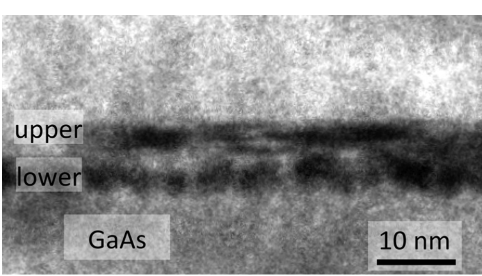

FIG. 4. High-resolution TEM image of the nanoparticle-seeded ErAs layer grown with 3.0 nm GaAs spacer. The two distinct nanoparticle layers (denoted lower and upper) correspond to the nanoparticle seed layer (lower) and the parasitic surface nanoparticle layer (upper).

erbium incorporation into GaAs to grow an ErAs layer through a thin GaAs spacer that maintains registration with the underlying GaAs substrate. Electrical measurements of temperature dependant conductivity are underway to observe a transition from hopping transport associated with nanoparticle layers to band like transport of films and will be reported elsewhere. Further development of the growth method is required to grow thicker ErAs films, and extension of the growth method to a lattice-matched semimetal/semiconductor system, such as ScErAs, will enable the integration of semimetallic films within optical devices.

The authors would like to thank Professor Paulo Ferreira for useful discussions. This work was supported by the Army Research Office (Grant No. W911NF-07-1-0528), and the Air Force Office of Scientific Research (Grant No. FA9550-10-1-0182), and the National Science Foundation (Grant No. ECCS-0954732).

[1]W. L. Barnes, A. Dereux, and T. W. Ebbesen, Nature **424**, 824 (2003).
[2]J. Vuckovic, M. Loncar, and A. Scherer, IEEE J. Quantum Electron. **36**, 1131 (2000).
[3]C. J. Palmstrøm, Annu. Rev. Mater. Sci. **25**, 389 (1995).
[4]C. J. Palmstrøm, N. Tabatabaie, and J. S. J. Allen, Appl. Phys. Lett. **53**, 2608 (1988).
[5]T. Sands, C. J. Palmstrøm, J. P. Harbison, V. G. Karamidas, N. Tabatabaie, T. L. Cheeks, R. Ramesh, and Y. Silberberg, Mater. Sci. Rep. **5**, 99 (1990).
[6]J. G. Zhu, C. J. Palmstrøm, and C. B. Carter, J. Appl. Phys. **77**, 4321 (1995).
[7]M. Grundmann, Phys. Status Solidi B **248**, 805 (2011).
[8]D. W. Elsaesser, Y. K. Yeo, R. L. Hengehold, K. R. Evans, and F. L. Pedrotti, J. Appl. Phys. **77**, 3919 (1995).
[9]I. Poole, K. E. Singer, A. R. Peaker, and A. C. Wright, J. Cryst. Growth **121**, 121 (1992).
[10]P. Rutter, K. E. Singer, and A. R. Peaker, J. Cryst. Growth **182**, 247 (1997).
[11]S. Sethi, T. Brock, P. K. Bhattacharya, J. Kim, S. Williamson, D. Craig, and J. Nees, IEEE Electron Device Lett. **16**, 106 (1995).
[12]H. Yamaguchi and Y. Horikoshi, Appl. Phys. Lett. **60**, 2341 (1992).
[13]K. E. Singer, P. Rutter, A. R. Peaker, and A. C. Wright, Appl. Phys. Lett. **64**, 707 (1994).
[14]N. Jourdan, H. Yamaguchi, and Y. Horikoshi, Jpn. J. Appl. Phys. **32**, L1784 (1993).
[15]C. Kadow, S. B. Fleischer, J. P. Ibbetson, J. E. Bowers, A. C. Gossard, J. W. Dong, and C. J. Palmstrøm, Appl. Phys. Lett. **75**, 3548 (1999).
[16]B. D. Schultz and C. J. Palmstrøm, Phys. Rev. B **73**, 241407 (2006).
[17]A. M. Crook, H. P. Nair, and S. R. Bank, Appl. Phys. Lett. **98**, 121108 (2011).
[18]A. Guivarc'h, Y. Ballini, Y. Toudic, M. Miener, P. Auvray, B. Guenais, J. Caulet, B. L. Merdy, B. Lambert, and A. Regreny, J. Appl. Phys. **75**, 2876 (1994).
[19]C. Kadow, J. A. Johnson, K. Kolstad, J. P. Ibbetson, and A. C. Gossard, J. Vac. Sci. Technol. B **18**, 2197 (2000).

Downloaded 15 Sep 2012 to 128.83.63.20. Redistribution subject to AIP license or copyright; see http://apl.aip.org/about/rights_and_permissions